– Supporting Information –

Unexpected plasticization effects on the structure and properties of polyelectrolyte complexed chitosan/alginate materials

Pei Chen [a,b], *Fengwei Xie* [b,c,*,†], *Fengzai Tang* [d], *Tony McNally* [b,**]

[a] College of Food Science, South China Agricultural University, Guangzhou, Guangdong 510642, China

[b] International Institute for Nanocomposites Manufacturing (IINM), WMG, University of Warwick, Coventry CV4 7AL, United Kingdom

[c] School of Chemical Engineering, The University of Queensland, Brisbane, Qld 4072, Australia

[d] WMG, University of Warwick, Coventry CV4 7AL, United Kingdom

[*] Fengwei Xie. Email: d.xie.2@warwick.ac.uk, fwhsieh@gmail.com

[**] Tony McNally. Email: t.mcnally@warwick.ac.uk

[†] This author leads the research.

Table of Contents

FIGURES S3
TABLES S6
NOTES TO FIGURES S7
REFERENCES S8

FIGURES

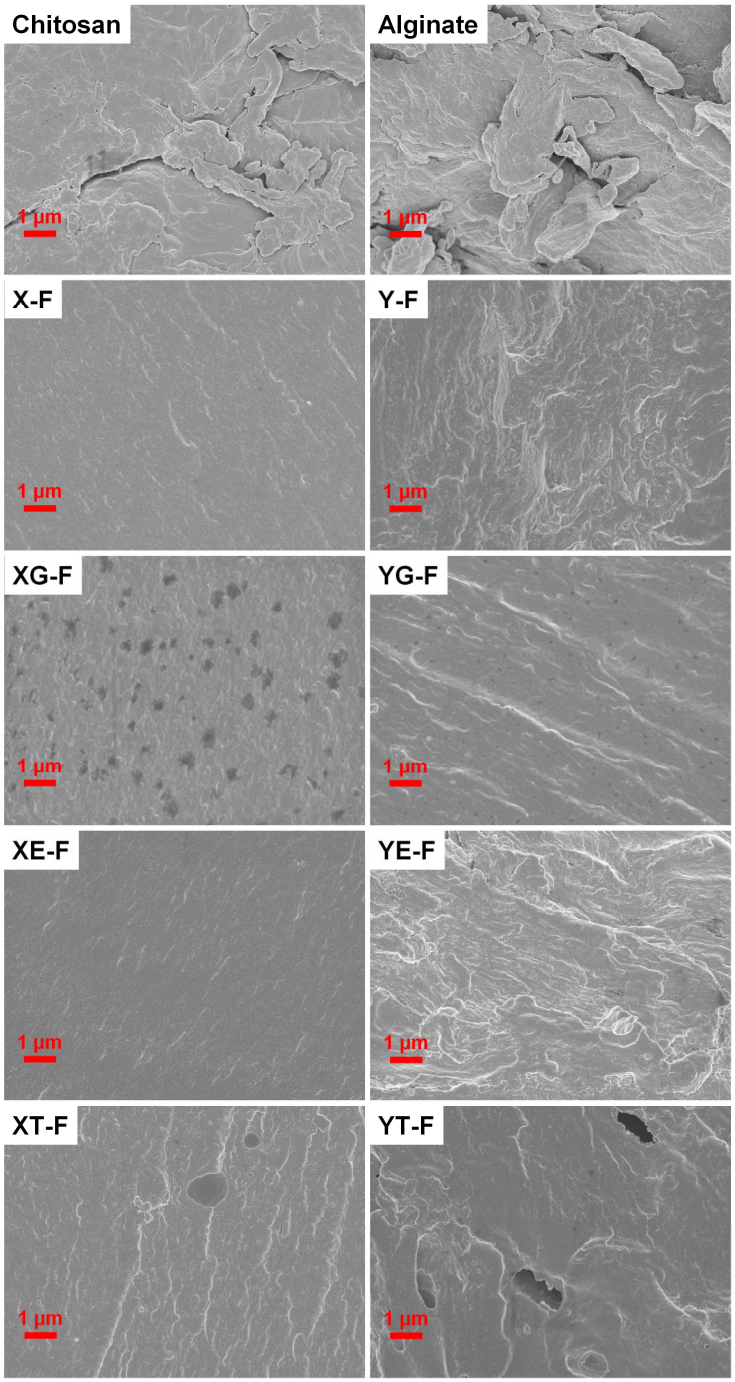

Figure S1. a) SEM images of cryo-fractured surfaces of the different biopolymer films.

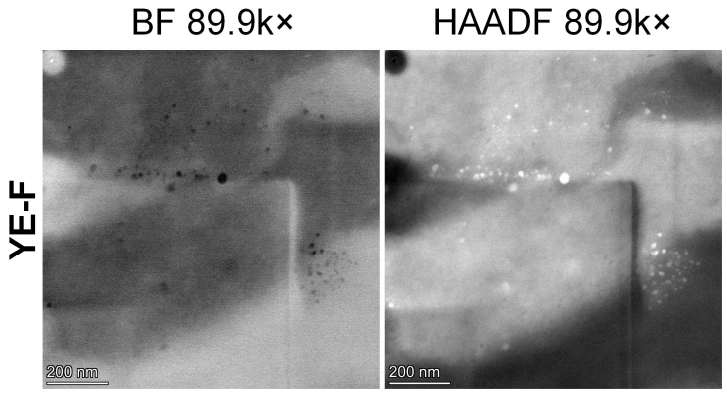

Figure S2. a) STEM images of YE-F. The "new structure" formed during STEM imaging are the black areas in the BF image or white areas in the HAADF image.

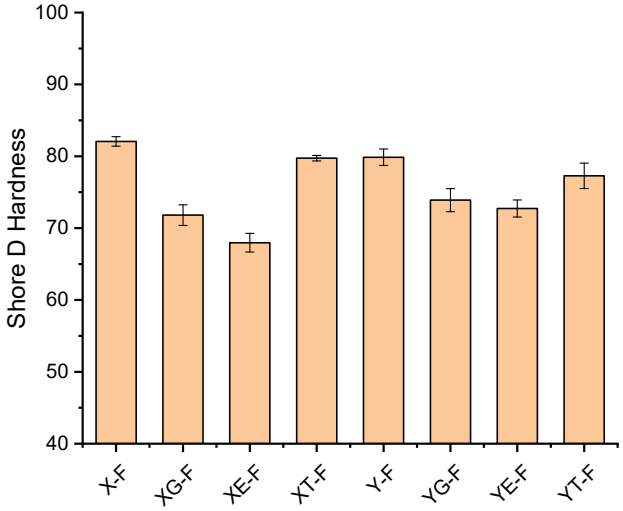

Figure S3. Shore D hardness of the different biopolymer films. Error bars represent standard deviations.

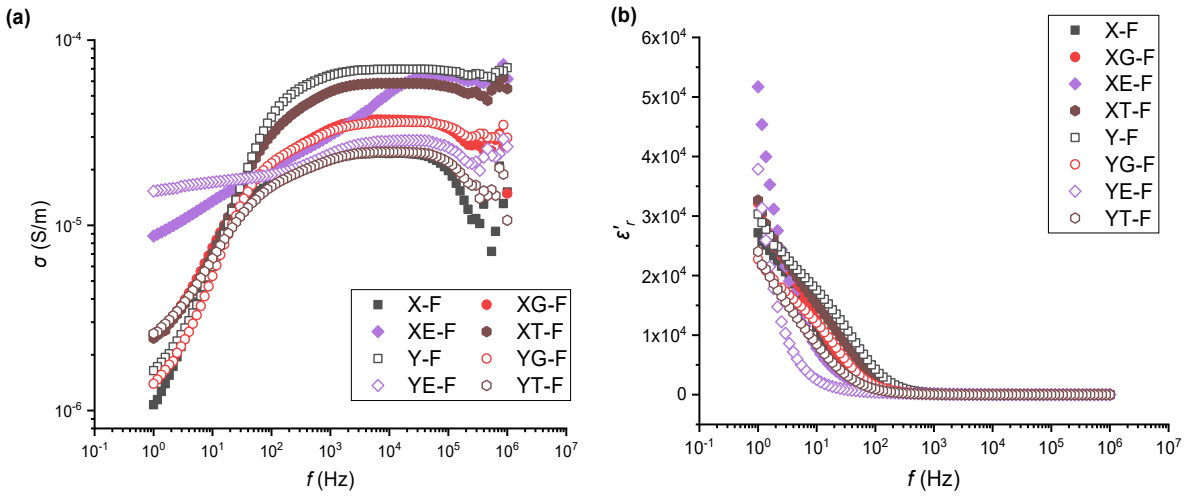

Figure S4. EIS results for the different biopolymer films: a) AC conductivity (σ); and b) real relative permittivity (ε'_r).

TABLES

Table S1. Bulk resistance (R_b) and ionic conductivity (σ_{dc}) calculated from the Nyquist plots of impedance, and real relative permittivity (ε'_r) at 1 kHz, of the different biopolymer films at RT.

Sample	R_b ($\times 10^4$, Ω)	σ_{dc} (10^{-5}, $S \cdot m^{-1}$)	ε'_r at 1 kHz
X-F	6.10±0.22	2.41±0.05	69±29
XG-F	3.57±0.60	3.93±0.70	130±27
XE-F	2.23±0.27	6.85±0.78	208±22
XT-F	2.02±0.24	6.21±0.78	182±34
Y-F	1.84±0.29	6.63±0.97	183±38
YG-F	2.80±0.31	3.65±0.41	103±43
YE-F	3.97±0.30	2.74±0.20	66±13
XT-F	5.21±2.30	2.29±0.94	64±37

NOTES TO FIGURES

In **Figure 3** (FTIR), chitosan displayed characteristic reflections at 1649 cm^{-1} (amide I), 1591 cm^{-1} (N─H bending from amine and amide II), 1420 cm^{-1} (vibration of O─H in the ring), 1375 cm^{-1} (CH_3 symmetrical deformation mode), 1319 cm^{-1} (vibration of C─H in the ring), 1265 cm^{-1} (amide III), 1190–920 cm^{-1} (C─N stretching), 1150–1040 cm^{-1} (asymmetric C─O─C stretching in the glycosidic linkage), and 1024 cm^{-1} (skeletal vibration of C─O stretching).[1-3] Alginate sodium exhibited peaks at 1591 cm^{-1} (asymmetric COO^- stretching), 1408 cm^{-1} (symmetric COO^- stretching), 1300 cm^{-1} (skeletal vibration of C─CH and O─CH bending), 1082 cm^{-1} (asymmetric C─O─C stretching in the glycosidic linkage), and 1024 cm^{-1} (skeletal vibration of C─O stretching).[1, 4]

In **Figure 4** (XRD), within the 2θ range examined, chitosan displayed two strong peaks as reported previously.[5-6] The peak at 13.2° 2θ ((020) reflection, *d*-spacing = 0.78 nm) is assigned to hydrated crystals due to the integration of water molecules in the crystal lattice and the peak located at 23.3° 2θ ((100) reflection, *d*-spacing = 0.44 nm) is attributed to the regular crystal lattice of chitosan.[7] Alginate exhibited two broad XRD peaks as observed previously.[8-9] The peak at 15.9° (*d*-spacing = 0.65 nm) is due to the (110) plane from the poly(guluronate) unit and the one at 25.1° (*d*-spacing = 0.41 nm) due to the (200) plane from the poly(mannuronate) unit.[10-11]

Figure S4(a) shows that for all the biopolymer films, AC conductivity (σ) increased with frequency (*f*), which is typical of an insulating material (dielectric). Nonetheless, XE-F and YE-F had higher σ values at low *f* (< 30 Hz) than the other samples. In this regard, with [C_2mim][OAc], it could be that more mobile ions in the bulk material contribute towards conductivity especially at low *f*.[12] **Figure S4**(b) shows that the real relative permittivity (ε'_r) of all samples increased abruptly with decreasing *f*, which could be associated with electrode polarization and space charge

effects (dipole moment).[13-14] For XE-F and YE-F, ε'_r increased more sharply with decreasing *f*. In these samples, the mobile ions could be contributed by [C_2mim][OAc].

REFERENCES

(1) Lawrie, G.; Keen, I.; Drew, B.; Chandler-Temple, A.; Rintoul, L.; Fredericks, P.; Grøndahl, L. Interactions between Alginate and Chitosan Biopolymers Characterized Using FTIR and XPS. *Biomacromolecules* **2007,** *8* (8), 2533-2541, DOI: 10.1021/bm070014y.

(2) Pawlak, A.; Mucha, M. Thermogravimetric and FTIR Studies of Chitosan Blends. *Thermochim. Acta* **2003,** *396* (1-2), 153-166, DOI: 10.1016/s0040-6031(02)00523-3.

(3) Chen, Z.; Mo, X.; He, C.; Wang, H. Intermolecular Interactions in Electrospun Collagen–Chitosan Complex Nanofibers. *Carbohydr. Polym.* **2008,** *72* (3), 410-418, DOI: 10.1016/j.carbpol.2007.09.018.

(4) Papageorgiou, S. K.; Kouvelos, E. P.; Favvas, E. P.; Sapalidis, A. A.; Romanos, G. E.; Katsaros, F. K. Metal–Carboxylate Interactions in Metal–Alginate Complexes Studied with FTIR Spectroscopy. *Carbohydr. Res.* **2010,** *345* (4), 469-473, DOI: 10.1016/j.carres.2009.12.010.

(5) Epure, V.; Griffon, M.; Pollet, E.; Avérous, L. Structure and Properties of Glycerol-Plasticized Chitosan Obtained by Mechanical Kneading. *Carbohydr. Polym.* **2011,** *83* (2), 947-952, DOI: 10.1016/j.carbpol.2010.09.003.

(6) Matet, M.; Heuzey, M.-C.; Pollet, E.; Ajji, A.; Avérous, L. Innovative Thermoplastic Chitosan Obtained by Thermo-Mechanical Mixing with Polyol Plasticizers. *Carbohydr. Polym.* **2013,** *95* (1), 241-251, DOI: 10.1016/j.carbpol.2013.02.052.

(7) Kittur, F. S.; Vishu Kumar, A. B.; Tharanathan, R. N. Low Molecular Weight Chitosans—Preparation by Depolymerization with *Aspergillus Niger* Pectinase, and Characterization. *Carbohydr. Res.* **2003,** *338* (12), 1283-1290, DOI: 10.1016/s0008-6215(03)00175-7.

(8) Gao, C.; Pollet, E.; Avérous, L. Properties of Glycerol-Plasticized Alginate Films Obtained by Thermo-Mechanical Mixing. *Food Hydrocolloids* **2017,** *63*, 414-420, DOI: 10.1016/j.foodhyd.2016.09.023.

(9) Gao, C.; Pollet, E.; Avérous, L. Innovative Plasticized Alginate Obtained by Thermo-Mechanical Mixing: Effect of Different Biobased Polyols Systems. *Carbohydr. Polym.* **2017,** *157*, 669-676, DOI: 10.1016/j.carbpol.2016.10.037.

(10) Sikorski, P.; Mo, F.; Skjåk-Bræk, G.; Stokke, B. T. Evidence for Egg-Box-Compatible Interactions in Calcium−Alginate Gels from Fiber X-ray Diffraction. *Biomacromolecules* **2007,** *8* (7), 2098-2103, DOI: 10.1021/bm0701503.

(11) Fabia, J.; Ślusarczyk, C.; Gawłowski, A. Supermolecular Structure of Alginate Fibres for Medical Aplications Studied by Means of WAXS and SAXS Methods. *Fibres and Textiles in Eastern Europe* **2005,** *13* (5), 114-117.

(12) Osman, Z.; Ibrahim, Z. A.; Arof, A. K. Conductivity Enhancement due to Ion Dissociation in Plasticized Chitosan Based Polymer Electrolytes. *Carbohydr. Polym.* **2001,** *44* (2), 167-173, DOI: 10.1016/S0144-8617(00)00236-8.

(13) Khiar, A. S. A.; Puteh, R.; Arof, A. K. Conductivity Studies of a Chitosan-Based Polymer Electrolyte. *Physica B* **2006,** *373* (1), 23-27, DOI: 10.1016/j.physb.2005.10.104.

(14) Navaratnam, S.; Ramesh, K.; Ramesh, S.; Sanusi, A.; Basirun, W. J.; Arof, A. K. Transport Mechanism Studies of Chitosan Electrolyte Systems. *Electrochim. Acta* **2015,** *175*, 68-73, DOI: 10.1016/j.electacta.2015.01.087.